JOURNAL OF MATERIALS SCIENCE 12 (1977) 75–89

Condensation of zinc aerosols

E. R. BUCKLE, K. C. POINTON*
Department of Metallurgy, The University of Sheffield, UK

Condensation of zinc aerosols in the presence of argon was studied in the heat-pulse cloud chamber; as with cadmium, two distinct series of particles are produced as the wall temperature is increased, first prisms and then spheres. The prismatic particles are mono-crystalline and include complicated dendrites and a species not previously seen, the capped prism. Whiskers grow from the basal surfaces of the simple prisms. The spherical particles include mono-, bi-, and poly-crystals.

The production of simple prisms and dendrites is attributed to condensation of solid in the presence of particularly steep temperature and vapour-pressure gradients. Crystallographic evidence supports the view that the spheres condense as liquid droplets. It is concluded that the droplets solidfy from nuclei that grow rapidly into circular {0 0.1} rafts on the liquid surface, in the manner observed with large sessile drops by Mutaftschiev and Zell. The formation of hillocks on the basal raft or its conversion into a concave dish is evidence of growth in the vapour.

The number n of basal rafts on a solidified sphere may be identified with the number of nuclei. When unimpeded by other nuclei, a raft grows to a maximum radius $r \sim 0.55\,R$, where R is the droplet radius. The ratio r/R is used to deduce the orientation of the pyramidal planes which develop at the edge of the raft as it begins to thicken. At low wall temperatures some of these planes tend to be very coarse, while when the growth front reaches the opposite side of the particle, the solid surface adopts a relatively smooth spherical outline.

As the wall temperature is raised, the highest value observed for n increases from 1 to a maximum of 20 to 30 and then falls abruptly as the melting point of the metal is approached. The temporary increase in n may be an effect of drop size but the final fall is ascribed to the failure of supercooled droplets to nucleate until withdrawn from the apparatus. Spheres with $n > 1$ deform on cooling as the result of thermal expansion anisotropy. For $n > 2$ cracking and slip are observed.

1. Introduction

The work of the present paper was a continuation of that described in previous publications [1, 2], and forms part of a systematic study of metallic condensation in which one of the main objectives is to explore the earliest stages of phase change. The rapid growth and motion of particles in surroundings at high temperatures makes it difficult to examine them while they are in process of formation, and so far it has been necessary to rely on indirect information gained by the study of the final sediment in relation to the conditions of generation. With the benefit of a considerable stockpile of information on Cd with which to make comparisons, it has proved possible to carry out the investigation of Zn more effectively. Although these metals were chosen primarily for their low melting points and high volatilities, the anisotropic crystal properties are a considerable advantage in the interpretation of particle structure.

* Present address: Edwards High Vacuum, Manor Royal, Crawley, Sussex.

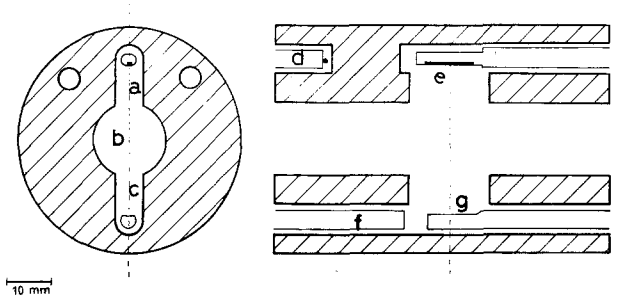

Figure 1 Cloud chamber: central section. a, vapour generation zone; b, circulation zone; c, collection zone; d, thermocouple; e, supersaturator (down operation); f, exhaust probe; g, substrate.

2. Experimental

Using the apparatus previously described [1], aerosols of Zn were generated by flash-heating the metal (99.999% purity) in Ar at a series of wall temperatures T_∞ (previously denoted by T) extending from laboratory ambient to a point 84 K above the melting point T_f (692.7 K). Particles were caught on a substrate and removed for examination in the same way as before.

Although our earlier conclusion that the final crystalline form is dominated by the wall temperature still held, the appearance of fall-out was to some extent sensitive to the procedure for generating vapour. The conditions of temperature and vapour pressure in the supersaturator slot (Fig. 1) could be varied by rotating the probe so that the groove holding the metal faced either up or down during use. These alternative positions will be referred to as the "up" and "down" positions. An advantage of down operation is that less heat is required to produce a cloud when the wall temperature is low ($T_\infty \sim 300$ K). This had been observed during the work on Cd, although problems were encountered in retaining the metal in the downward-facing groove which restricted such experiments to room temperature. In the present work, the groove could be held inverted during operation with T_∞ up to 0.83 T_f. The effects of the change from down to up operation were less obvious above 0.7 T_f.

3. Results and discussion

The results with Zn broadly resembled those obtained with Cd, and in this paper we present new information obtained with the benefit of the modified generation procedure, and we extend the interpretation of aerosol behaviour by considering the main body of results for both metals.

3.1 Types of particles in Zn fall-out

Morphological charts for the various particle types are given in Fig. 2. Most of the types were described in a previous paper [1]. Comparison of the Zn charts with those of Cd reveals a tendency for particles of a given type to grow somewhat larger in Zn aerosols at a given wall temperature. This is as expected from the densities and vapour pressures ($\rho_{Zn}/\rho_{Cd} = 0.82$ (melts) and $p^{\bullet}_{Zn}/p^{\bullet}_{Cd} = 1.5$ at $T = T_f$). As with Cd, precipitates collected at temperatures over most of the range up to T_f were evidently crystalline before landing on the substrate, the form changing from prismatic to spherical with increasing T_∞. The proportion of prisms was higher in down operation, although when the supersaturator was up their surfaces showed a greater degree of perfection (Fig. 3a) and their temperature range was narrower (Fig. 2). The skeletal and dendritic forms of prisms occurred only in down operation (Fig. 3b and c). These were rarer, and tended to be bigger, than the simple prisms but existed over the same T_∞-range.

3.1.1. Capped prisms

Prismatic forms not observed in the Cd work are shown in Fig. 3d and e. Encountered only in down operation, they differed from simple prisms in possessing roughly-stepped spherical caps topped by small basal hexagons. The version capped at both ends was the more frequent, and although crudely spherical it differed from spheres as a class in never being smooth or having a circular outline to one of the basal faces. The temperature range matches that of simple prisms and dendrites but the size range is closer to the prisms' and they were much rarer than either species.

3.1.2. Spherical bi-crystals and flattened droplets

The spheres showed the same general trends as before, single crystals heavily outnumbering spheres with two or more crystallites under all conditions (Fig. 2). In down operation it was noticed with Zn that the surface texture of a sphere with two basal flats was equivalent to that

of two spherical monocrystals adhering together at a grain boundary (Fig. 4a and b). The spherical bicrystals were succeeded by polycrystals (Fig. 4c) as T_∞ was increased, although they maintained higher concentrations with the supersaturator was down. This was apparently connected with the fact that droplets solidified at a given T_∞ were smaller in down operation (Fig. 2F).

Sintering of adjacent spheres occurred frequently on the substrate when T_∞ exceeded 0.9 T_f, but flattening, indicative of molten particles, failed to occur even at $T_\infty > T_f$ until the silica substrate was replaced by one of Zn cooled [2] to $T_\infty -$ 56 K. Drops smaller than 3 μm then showed distortion as the result of adhesion to the substrate (Fig. 4d). The successful demonstration of the molten state of such small particles depends on the complex interplay of heat transfer, surface tensions, viscous relaxation and momentum. This is becoming a familiar problem in connexion with "splat-cooling" [3].

3.2. Particle morphology and condensation mechanisms

The change-over from prisms to spheres with increasing wall temperature is suggestive of a change of condensation mechanism. A similar conclusion was reached some time ago when dendrites were observed in aerosols of certain volatile metallic salts [4]. Further evidence is given by Fig. 2A to D. It would be expected that under given conditions liquid would condense more rapidly than solid, and the charts show that the size ranges of the prismatic particles contracted as droplets took over. The possibility of such a change in mechanism was recently discussed in relation to the principles of boundary-layer condensation [5]. Briefly, it is postulated that the change from prisms to spheres corresponds to a replacement of solid by liquid as the state in which material first condenses from the vapour. This is theoretically possible if the threshold of condensation occurs at a point in the vapour-rich boundary layer at which the local temperature is at first below T_f but increases through T_f as the external temperature, T_∞, is raised. It has not yet been verified that the physical properties of Cd and Zn meet the theoretical requirements, and in this paper we shall discuss only the morphological evidence obtained with the cloud chamber and other experimental techniques.

3.2.1. Prismatic particles

The total pressure in the cloud chamber is virtually equal to atmospheric at all temperatures [2]. This limits the temperature of the vapour source to the boiling point of the metal. Progression through the prismatic series of particles with increasing T_∞ therefore coincides with a continuing reduction in the extremes of temperature which the vapour can experience on the way to the circulation zone. It is of interest to enquire whether under these changing conditions the crystalline form develops in the way expected from the results of other work.

In their skeletal form (Fig. 3b), prisms show a tendency to grow in directions normal to pyramidal planes, $\{1\,1.l>0\}$. These are also the directions adopted by the dendrites. The growth structure, however, appears to consist of massive $\{1\,0.0\}$ steps on $\{0\,0.1\}$ surfaces, or vice versa (this is also the case on the $\{1\,0.l\}$ surfaces of spheres). It is possible that the angles between the dendrite arms and the principal crystal axis are subject to strain, for example, through the deposition of the Au–Pd protective coat, particularly in delicate forms like that of Fig. 3c. The winged individual of Fig. 3f has achieved a firmer structure with prominent basal flats. The similarity between this particle and others such as the skeleton of Fig. 3b and the hopper crystal of Fig. 3g suggests that a central nucleus grows arms which later merge to produce hollow basal faces. Perfection of the form requires the filling-in of $\{1\,0.0\}$ and $\{0\,0.1\}$ surfaces.

That dendritic growth may be a stage in prism development is suggested by several observations. As T_∞ is raised the smaller prisms are the first to perfect their faces, and the largest prisms are of a size comparable with that of the largest dendrites. The absence of dendrites as the result of up operation indicates that perfection of the prismatic form is sensitive to the boundary-layer conditions in the supersaturator slot. An increase in T_∞ in down operation is thus equivalent to a change to up operation.

Features of the capped prism suggest a change of growth mechanism. It is now the pyramids of the second type [6], $\{1\,1.l\}$, that are cavernous rather than the $\{1\,0.l\}$ pyramids of the skeletal prism. The ill-formed pyramidal prisms of Fig. 3h resemble singly and doubly capped prisms, and the failure of capped prisms to outgrow or displace the

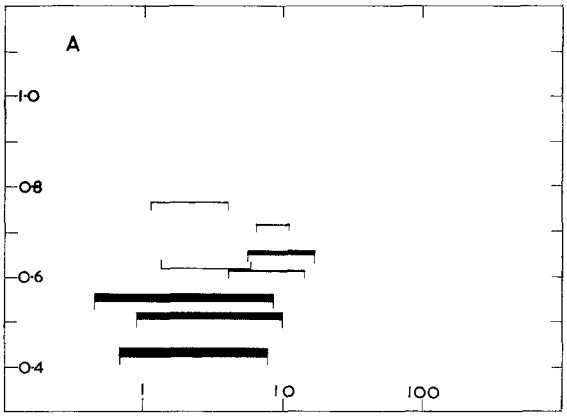

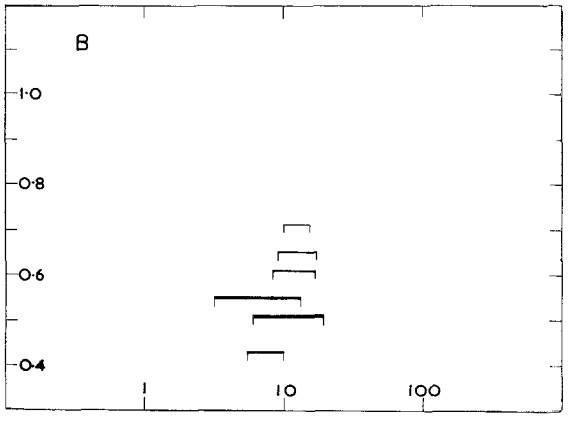

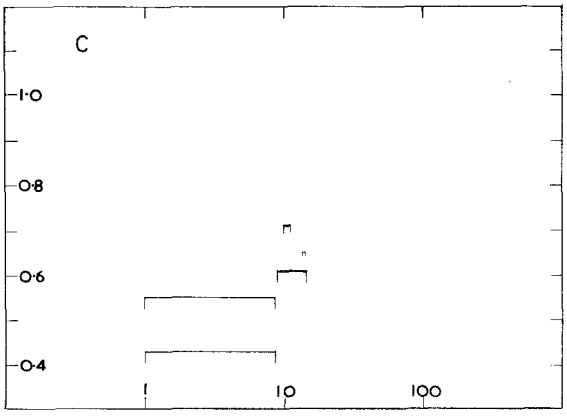

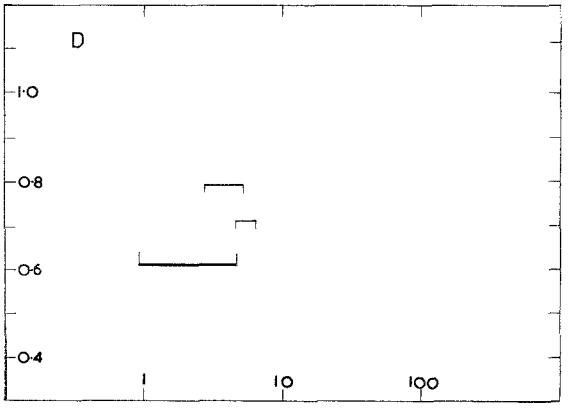

Figure 2 Morphological charts (⌊⌋= up, ⌈⌉ = down). Ordinate: T_∞/T_f. Abscissa: log (diameter/μm). Linewidth: population fraction. (A) simple prisms; (B) dendrites; (C) capped prisms; (D) pyramidal prisms; (E) spherical monocrystals; (F) multi-dished spheres; (G) spherical polycrystals; (H) smooth spheres.

Figure 2 continued.

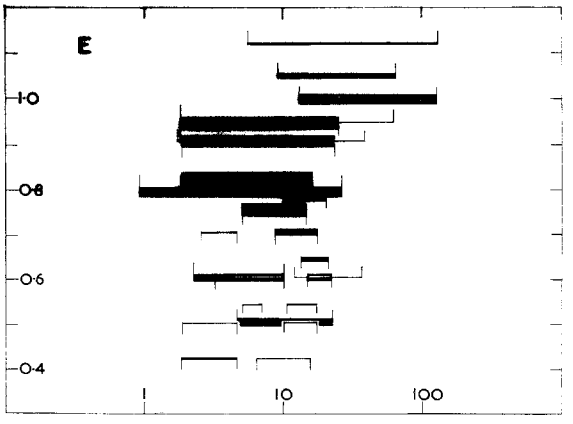

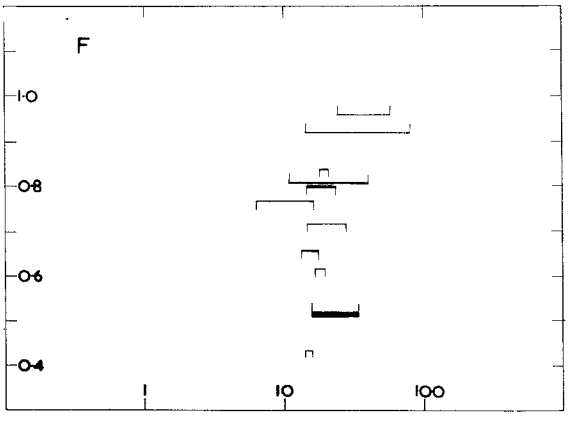

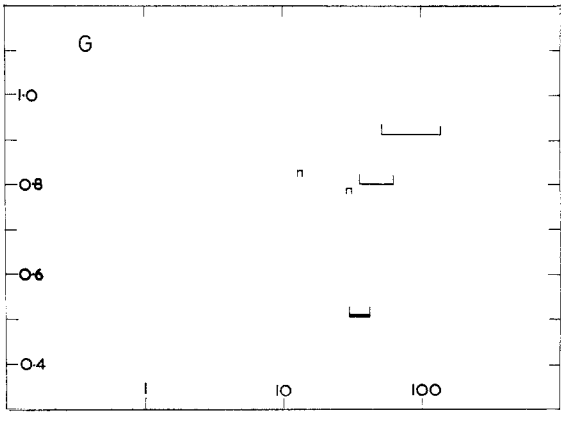

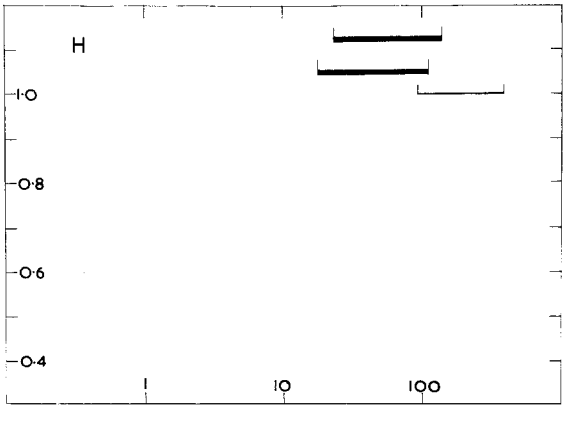

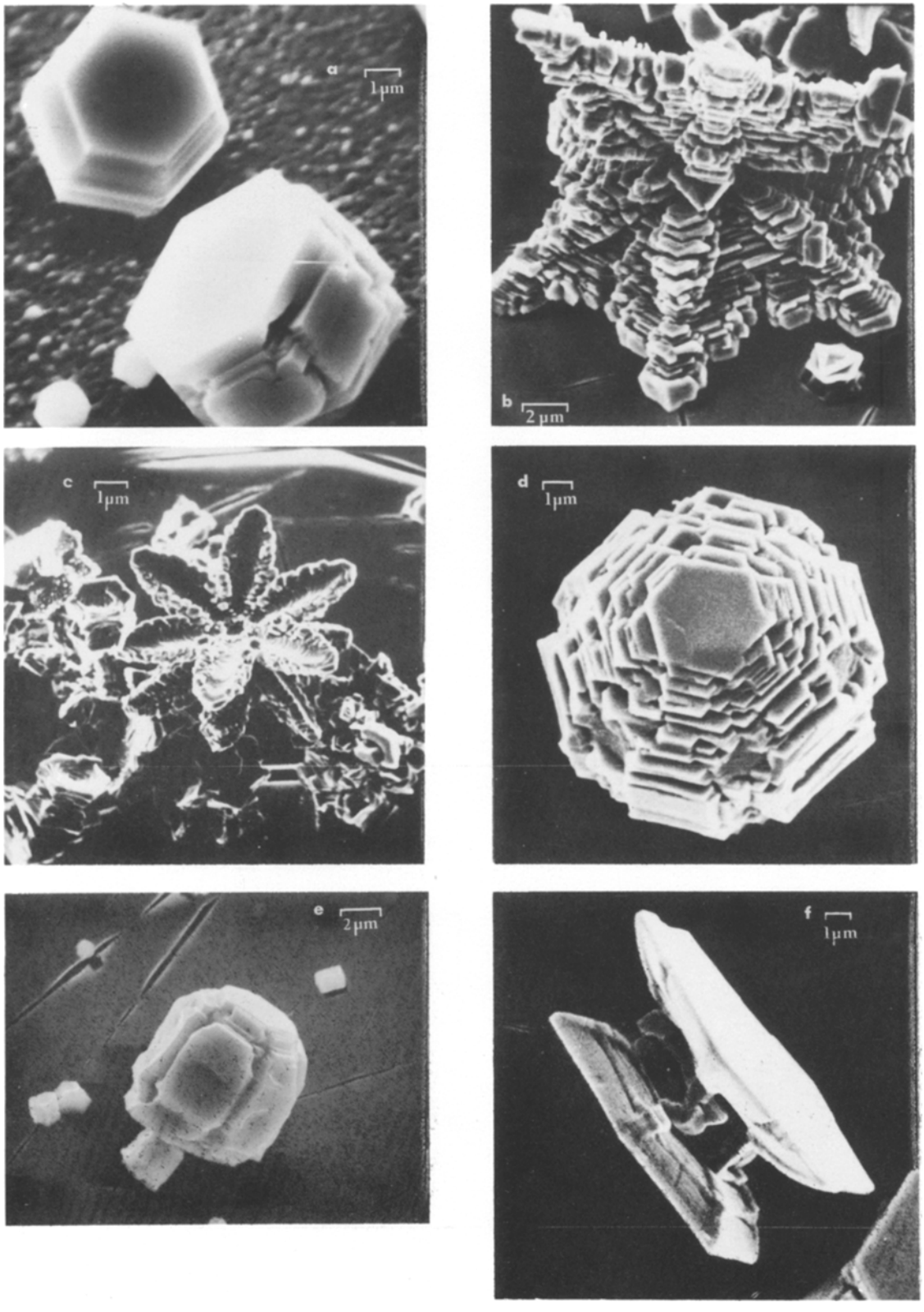

Figure 3 Prismatic particles (T_∞/T_f in parentheses; u = up, d = down): (a) 0.61d, (b) 0.51d, (c) 0.55d, (d) 0.65d, (e) 0.55d, (f) 0.65d, (g) 0.51d, (h) 0.71d, (i) 0.61u, (j) 0.61u, (k) 0.43d, (l) 0.61d.

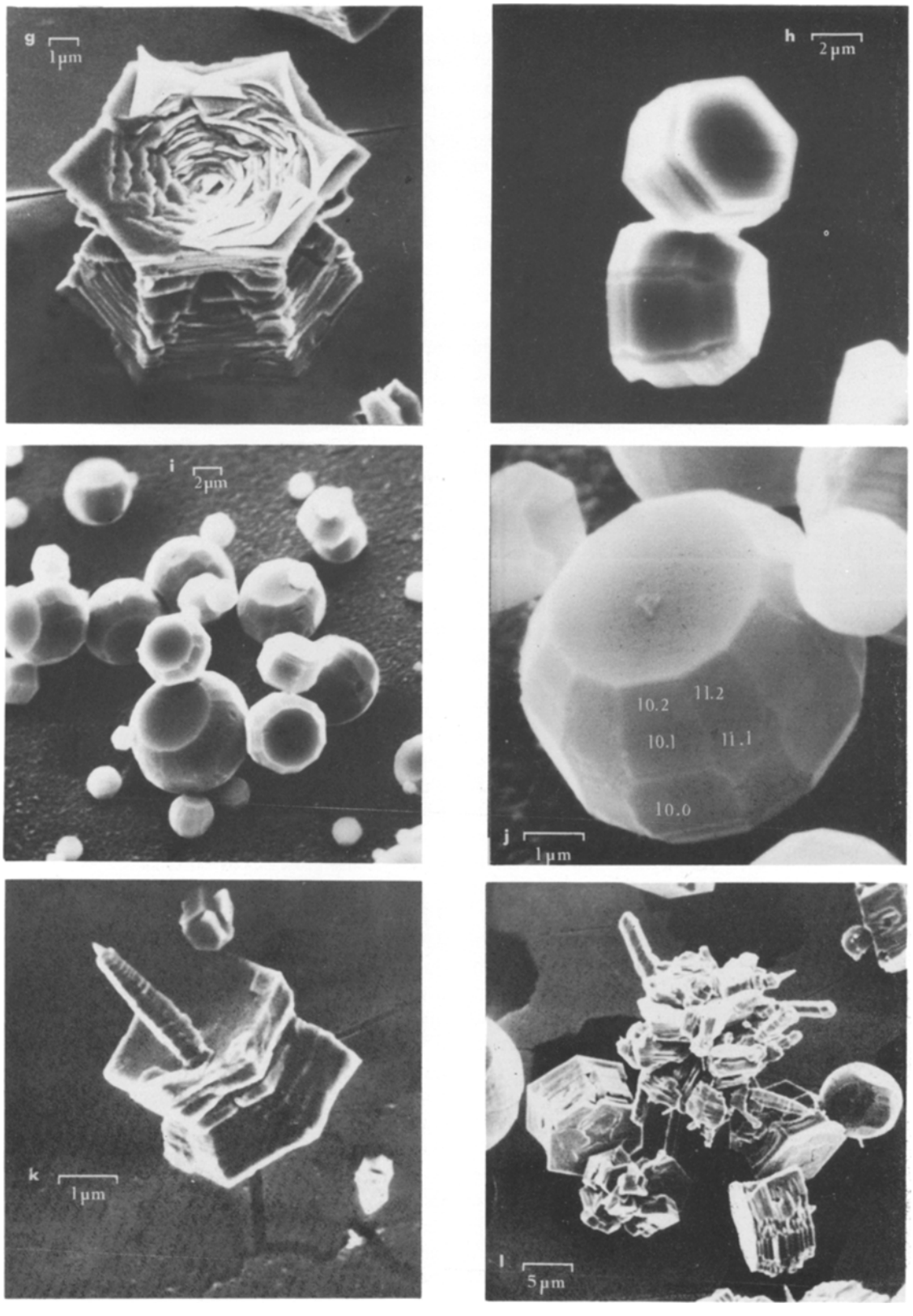

Figure 3 continued.

other prismatic forms would be explained if they were an intermediate form whose growth involved the slow development of pyramidal planes.

Distinction of well-formed pyramidal prisms and spherical monocrystals is relatively easy. Both basal flats on the prism are large and have clear hexagonal outlines. On the spheres produced at low temperatures only a small hexagonal flat occurs opposite the characteristic basal raft or dish, which is never a hexagon. In the less well developed pyramidal prism, residual cavities in the type II pyramidal areas sometimes produce indentations in the corners of the basal hexagons, giving them a polygonal appearance. A field showing the resemblance between these prisms and spherical monocrystals is given in Fig. 3i. The spheres can be recognized by their appearance in Fig. 3j.

A number of other investigators have published descriptions of particles from Zn condensation aerosols [7–14]. Details of the growth mechanisms have not been discussed in relation to the conditions of formation in these other sources, but there are some useful parallels between our observations and those of Heyer, *et al.* [15] and of Kaishev and Nanev [16]. These workers describe effects observed microscopically when millimeter-sized spheres of Zn, produced by distillation on to a cooled surface, are melted, re-frozen and then exposed to various temperatures and vapour supersaturations. The first evidence of solidification is the appearance of a basal flat. Facets develop round the flat until the particle has assumed the dynamic equilibrium form, namely, the form it maintains during subsequent growth under constant conditions.

The early history of such a particle is more relevant to a sphere than a prism, and this aspect will be pursued below. Of interest at this point are the relative stabilities reported for the pyramidal and prism faces under various conditions in the later stages of growth in the vapour. Kaishev and Nanev refer to experimental work in support of their prediction that as the temperature difference between the particle and the source of vapour is increased through the value 2.1 K, the pyramids $\{1\,1.1\}$ and $\{1\,1.2\}$ of the second type ($k = 1$) must grow out of existence. Their own experiment showed that above 7.1 K of undercooling the $\{1\,0.2\}$ and $\{1\,1.0\}$ facets also disappeared to leave the form $\{0\,0.1\} + \{1\,0.0\} + \{1\,0.1\}$ that we observe and classify as pyramidal prisms (Fig. 3j may be consulted for indexing of faces). A problem in matching their conclusions with our results is apparent in that when we lowered T_∞, the capped prism with its rough type II pyramids remained after the prism with only type I pyramids (the pyramidal prism) had disappeared (Fig. 2).

However, the *sequence* in which faces evolve on a particle in our experiments will be affected by the changing conditions in the boundary layer, through which it moves rapidly. The wall temperature T_∞ influences these conditions but will only lead to the assumption of the corresponding equilibrium shape if the particle spends enough time in the steady conditions of the circulation zone (Fig. 1). In this zone the vapour pressure is relatively small.

The influence of vapour pressure was studied over long periods by Heyer *et al.*, who noted that the $k = 1$ pyramids were persistent and rough, containing sub-facets of $\{0\,0.1\}$ and $\{1\,0.1\}$, at low temperatures when the supersaturation was also low but became smoother and eventually gave way to $\{1\,0.1\}$ pyramids at higher supersaturations. On this evidence, the capped prism will be preferred to the pyramidal prism ($k = 0$) when growth ends at low temperatures but relatively mild supersaturations. This supports the conclusion reached earlier based on the comparison of dendritic and capped growth-forms. The simple prism was not observed by these other workers and appears to be a form stable only under the high supersaturations of our aerosol experiments, where type I pyramids also grow out of existence.

3.2.1.1. Whiskers and prism clusters. A fairly rare development of the simple prism which occurred only in down operation is shown in Fig. 3k. The orientation and convex outline of the long process distinguishes it from the usual dendrite arm, and it was apparently a whisker. Such whiskers were also found detached from prisms and they apparently left behind flat hexagonal platforms on the basal faces of them (Fig. 3k). Low hillocks of this appearance might grow by surface nucleation if the surface of the prism was very smooth but the length of the whiskers suggests that they, and the hexagonal bases, originated from the emergence on the basal faces of screw dislocations with Burgers vector parallel to c [17]. Nanev and Iwanov [18] have described whisker growth on macroscopic Zn crystals. Whiskers were occasion-

ally found associated with aggregates of prismatic particles, or prism clusters. These clusters may have formed in suspension, as cases were found of clusters bristling with whiskers in all directions (Fig. 3l).

3.2.2. Spherical particles

In addition to the spreading of particles on the substrate at wall temperatures approaching T_f, new crystal-growth evidence strengthens the previous conclusion that the spheres are solidified droplets. This conclusion was based mainly on the occurrence of the basal dish and its striking ability to persist when the particle grows in the vapour. A circular flat was seen by other workers to form when drops of molten Cd or Zn froze, and it was reported to be extremely smooth [15, 16, 19]. With Zn it was again observed that when the supersaturator faced upwards, the dish, which begins as a flat, failed to develop a resolvable growth structure like the rest of the particle but merely became raised at the rim. As T_∞ approached T_f this hollowing was promoted and once again there appeared a non-metallic impurity, possibly oxide, on the dish which failed to receive a coat of Au–Pd and, therefore, became electrically charged in the beam of the SEM.

The area surrounding the dish was convex and at low temperatures it tended to be very rough. In the low but fairly uniform supersaturations of the circulation zone, nucleation and growth from the vapour was preferred on stepped areas in which the underlying structure is close-packed. The prisms and pyramids of type I developed readily, as shown by the high, straight ledges (Fig. 4e). Planes of type II filled in by accumulation of end facets of ledges lying in planes of type I. The type II planes were severely cavitated when T_∞ was low but gradually became smoother as it was raised.

With the supersaturator down, the basal flat remained a permanent feature of the solidified sphere but showed evidence of growth at all temperatures investigated up to 0.71 T_f. At these temperatures the flats frequently possessed low hexagonal or trigonal hillocks like those seen on prisms. Some hillocks gave the impression of a focus of growth activity near a corner (Fig. 4f) and the side-walls were pyramidal planes but there was never any sign of dendrites or whiskers attached to the spheres.

At the lowest temperatures the hillocks on a flat tended to be small and equal in size, and to occupy positions clear of the perimeter. The edges of neighbouring hillocks were sometimes collinear (Fig. 4f). As T_∞ was increased there was a general increase in size, and the largest hillocks occupied considerable lengths of perimeter. Eventually a point was reached where they became comparable in area to the flat itself and were no longer distinguishable. It appears that the basal flat fails to become dished because in down operation there is less restriction on two-dimensional nucleation and lateral growth. The increase in hillock size and decrease in number at high T_∞ points to the acceleration of growth.

3.3. Solidification, growth and evaporation of spherical monocrystals

Having discussed the condensation of spheres and prisms we now describe the geometrical and other characteristics attributable to the solidification of droplets and their subsequent growth or evaporation and discuss possible mechanisms.

3.3.1. Crystallography of the basal raft

When sessile drops of Cd and Zn are allowed to nucleate spontaneously, a basal flat first forms at a point on the surface opposite to that at which heat is extracted [15, 19]. Mutaftschiev and Zell found that the flat formed a floating raft*, and it would seem that the sensible and latent heat was conducted away from below the raft as it thickened. The airborne droplet has no substrate, and it is, in principle, possible for heat transfer to be controlled by an external process such as conduction, convection, radiation or volatilization which approximates to radial symmetry. Nevertheless, since our droplets resembled the sessile drops in the upper hemisphere after solidification, it is of interest to compare them geometrically.

Measurements on micrographs showed that with Zn monocrystals deposited at $T_\infty > T_f$, the value of the ratio r/R, where r is the radius of the basal flat and R the maximum radius of the convex spherical surface, was within 5% of 0.55. This gives 56° 30′ for the angle ψ in Fig. 5, assuming the convex surface of the measured particle to be

* It is stated in [19] that melt was only present initially above the raft when this was nucleated heterogeneously inside the drop, not, as we quoted in [1], when it nucleated spontaneously at the surface.

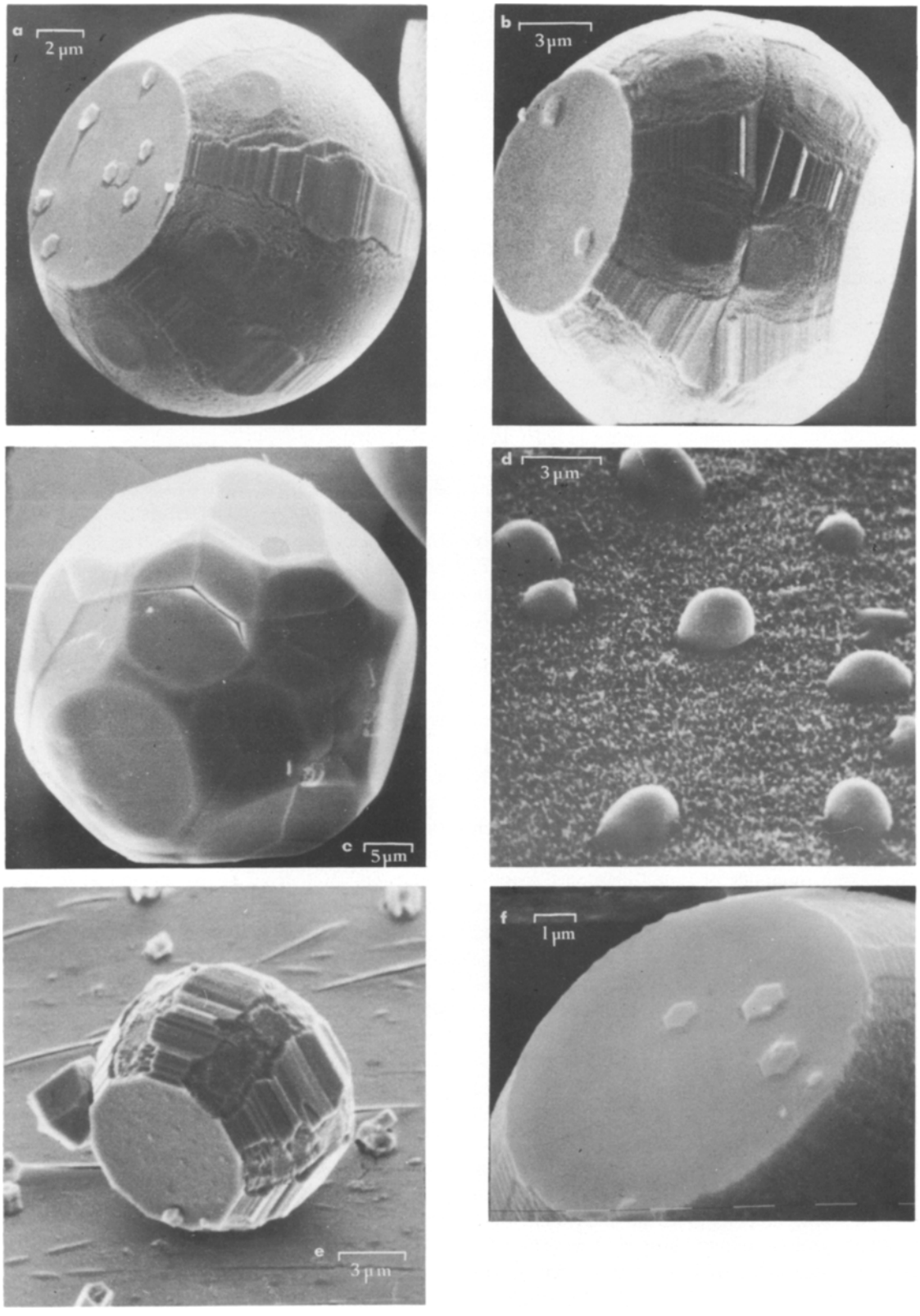

Figure 4 Spherical particles (T_∞/T_f in parentheses; u = up, d = down). (a) 0.61d, (b) 0.65d, (c) 0.80u, (d) 0.98u, (e) 0.55d, (f) 0.61d, (g) 0.76d, (h) 1.00u, (i) 1.00u, (j) 0.76d, (k) 0.80u, (l) 0.51u.

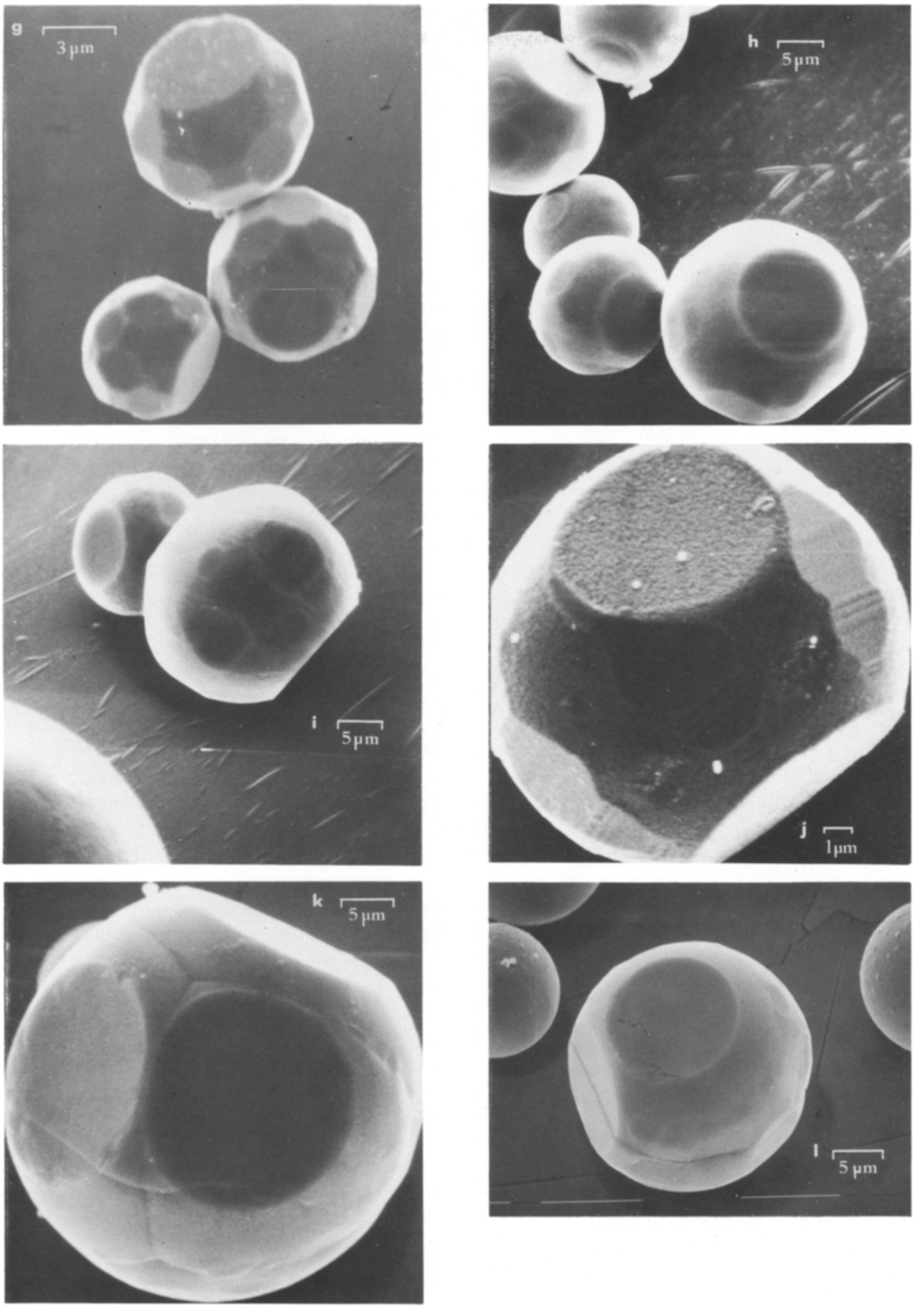

Figure 4 continued.

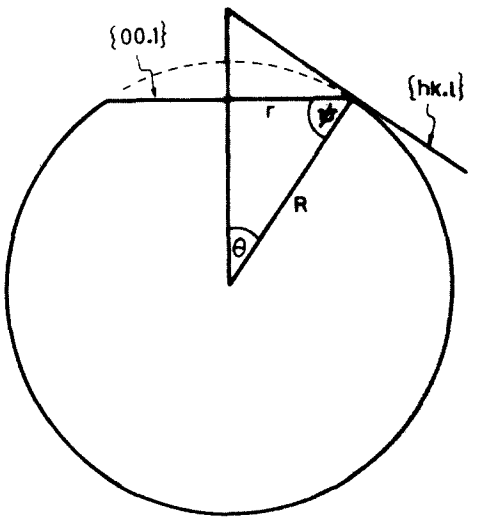

Figure 5 Geometry of the basal raft.

truly spherical. The assumption appears to be a good one for these spheres, which are smooth in outline. Anisotropy of the thermal expansion [20] results in a contraction of 6% in directions parallel to the basal flat and 2.7% in directions normal to it. No error is incurred if R is measured in a direction parallel to the direction of measurement of r, but the maximum error is otherwise only a 2% overestimate in the value of r/R.

According to Mutaftschiev and Zell's measurements, the value of ψ is $143 - 90 = 53°$ at the floating raft, independent of the drop size although increasing somewhat with the solidification rate. These are apparently the only values available. The authors consider the angle to be a function of the interfacial forces acting on the raft, and they also conclude that the formation of a flat face on the drop surface shows that it is not wetted perfectly by the melt. Other factors, such as hydrostatic forces resulting from the specific volume change and the slight temperature gradient may also affect the buoyancy of the growing nucleus. In our suspended droplets there is also a possibility of internal circulation caused by aerodynamic drag during the early history of the droplet, when it is moving rapidly through the condensation zone.

Heyer *et al.* [15] state that goniometry of the inclination of the type II pyramid to the prism face on Zn monocrystals gives $\psi = 55° 1'$ (Salkovitz [21], incidentally, gives exactly the same value for the angle between the basal face and the type I pyramid, 20.3). By the geometry of Fig. 5 and the general crystallographic relation [22] for $\tan\theta$ it may be shown that the indices of the pyramids with $k = 0$, h, respectively and which make contact with the basal flat at its periphery are related to r/R by

$$h/l = (r/R)/(2/\sqrt{3})(c/a)(1 - r^2/R^2)^{1/2},$$

$$h/l = (r/R)/2(c/a)(1 - r^2/R^2)^{1/2}.$$

From these expressions and the value 0.55 for r/R one obtains 0.30 and 0.18, respectively, for h/l. Heyer *et al.* consider the type II pyramid to be $\{2\,2.5\}$ or even $\{3\,3.8\}$ whereas the above value for h/l conforms more closely to $\{1\,1.6\}$. For type I a somewhat poorer fit to h/l is obtained with $\{1\,0.3\}$. Micrographs of Cd particles taken during the previous investigation [1] indicate that r/R may be nearer 0.53 for this metal, which has a larger axial ratio [21]. This figure is, however, based on relatively few measurements.

The value of 0.55 taken above was for Zn spheres that froze on the substrate after withdrawal from the hot chamber. The basal face is flat and the convex surface smooth on such a sphere because there has been no change after solidification.* The angle ψ on a sphere solidifying inside the chamber may be sensitive to T_∞ in view of the connection of T_∞ with the solidification rate. A survey of micrographs revealed that as T_∞ was raised from room temperature the ratio r/R rose to values as high as 0.68 and fell again to as low as 0.52 before finally adopting the value for the smooth, spherical monocrystal. At the same time, the surface texture changed, passing through a stage in which the outline became angular and the particles had a polyhedral appearance. At this stage the $\{1\,1.0\}$ prisms and $\{1\,0.1\}$ pyramids were the dominant non-basal faces and the basal flat remained circular in outline (Fig. 4g). The axial symmetry still distinguished these particles from polycrystals. Before the polyhedral stage the particles were spherical and rough, and after it they were spherical and smooth.

Measurement of R became somewhat arbitrary when the spheres were polyhedral, slightly different values being obtained depending on the orientation of the non-basal facets with respect to the direction of measurement across the outline. In view of

* The smooth spheres of Fig. 2H were entirely featureless (see also Table I, k of [1]).

this and the possible alteration of ψ with T_∞ it would seem inadvisable at present to attempt to relate variations in r/R with growth or evaporation after freezing. The hollowing of the basal flat when T_∞ is increased in up operation shows [1] that growth on it is retarded relative to growth on the surrounding surface under these conditions. This kinetic effect might not be inherent in the metallic structure, however, since in a torsion-effusion study on a macroscopic prism a slowing in the evaporation rate from the basal surface was suspected of being connected with the presence of residual O_2 in the evacuated container [23]. Contaminating gases might, for example, be released from the walls in the supersaturator zone during the more drastic heating in up operation.

3.3.2. *Final stages of solidification*

Persistent "tree-rings" [1] opposite the basal flat were observed with Zn. As the polyhedral sphere evolved into the smooth sphere with increasing T_∞, the last remnant of the rings was sometimes visible as a groove (Fig. 4h) of external radius rather less than that (r) of the opposite basal flat, although larger than that of the hexagon on a particle of the same size produced at low T_∞. The groove was sometimes wide and shallow, giving the impression of a small circular flat surmounted by a low dome. The profile then had the appearance shown in Fig. 4i, but even in this orientation its smooth outline distinguished it from the pyramidal prism, which also has two parallel flats.

The tree-rings are not found with polycrystals, and could be connected with the later stages of solidification from a single raft. The structure would suggest that the raft grows out into the droplet by the spreading of layers on the submerged basal plane (lateral growth mechanism). As the layer emerges from the melt the conditions at the growing ledges become affected by the temperature and pressure gradients in the vapour, and at high T_∞ their angularity is blunted by a small amount of growth in the vapour.

3.4. Solidification of spherical polycrystals

The relative positions of basal flats in polycrystalline spheres, including bicrystals, were apparently subject to chance. The mismatch of the growth structures at grain boundaries could be clearly seen in the surface detail of particles condensed at low T_∞ (Fig. 4b). If it may be assumed that a nucleus always grows into a floating raft, then it follows that each crystallite possesses a basal surface plane lying in the surface of the solidified droplet. The number of nuclei can, therefore, be counted under the microscope.

Measurement of the angle corresponding to the angle ψ at the floating raft was attempted on micrographs of solid particles in which a flat was in profile, but R could not be estimated very satisfactorily and r/R values were consequently not reliable. The rough estimates gave angles in the range observed on monocrystals provided measurement was made on a flat which had achieved the full size for the given droplet radius. Rafts apparently grow to their maximum size in the melt when they are not impeded, as was the case in the particle of Fig. 4j, by another raft or the growth front from another raft. The maximum size is not dependent on the presence of a large excess of melt because the structures show that it is achieved before the raft has thickened substantially. This agrees with the evidence of Mutaftschiev and Zell [19], and, with the absence of tree-rings, it appears to dispose of the possibility [1] that the nuclei grow outwards from the middle of the droplet to terminate in basal rafts. As with the spherical monocrystals, therefore, the size of the raft is connected with the curvature of the liquid surface, and this is supported by the estimates of the angle ψ, so far as they go.

Certain information about the timing of successive nucleations in a given droplet is revealed with the aid of this conclusion by examining bicrystals and other polycrystals which have a small number of basal flats separated by the residual curved surface (the "multi-dished sphere" of [1]). The small raft of Fig. 4j, for example, had no territory of its own outside the perimeter because it was engulfed by another growth front before it could attain full size. This raft was presumably nucleated at a late stage in solidification. The dishes and grain boundaries in Fig. 4k are in haphazard orientation, indicating that the grains had independent origins in time and position. In Fig. 4b, however, the particle is nearly symmetrical about the grain boundary, so that in this case solidification in the two halves must have occurred nearly simultaneously.

With polycrystals in general, the highest number of nuclei per droplet, $n = n_{max}$, slowly increased with T_∞ to between 20 and 30 and then fell rapidly at about $T_\infty = 0.95\, T_f$ because the droplets

failed to nucleate at all while inside the chamber. Although nucleation must cease as T_∞ approaches T_f, it is not obvious why n_{max} first increases. It is possibly a size effect. The nucleation and growth rates both increase with the extent of supercooling, $T_f - T$, but nucleation is the more sensitive process and sets in at a threshold T_s for which the supercooling $T_f - T_s$ is substantial [24]. Consequently, once formed the nucleus grows rapidly and the droplet recalesces to a temperature above the threshold, and further nucleation is prevented. If the rafts nucleate spontaneously at the surface they will do so at a rate proportional to R^2, so that small drops tend to develop few nuclei during their brief excursion below T_s in the molten state. Apart from droplets condensed at $T_\infty > 0.95\ T_f$, which nucleated on withdrawal, monocrystalline spheres were smaller than the vast majority of polycrystalline ones (Fig. 2F), and of the polycrystals those with more numerous nuclei were the larger (Fig. 2G). This supports the spontaneous nucleation mechanism. The cut-off of polycrystals and the corresponding jump in size of spherical monocrystals puts T_s very roughly at $0.95\ T_f$ (Fig. 2), which is rather higher than the figure for Cd [1].

A tendency for molten particles to freeze to polycrystals at high T_∞ and monocrystals at low T_∞ was observed during work on the salt PbI_2 [25]. The "twinkling" seen in salt aerosols was sometimes strong enough for the moment of solidification to be detectable by eye. This was not possible with the metals [2]. However, since growth of hillocks on the basal flat was sensitive to the attitude of the vapour source in the generation zone (Fig. 1), it may be concluded that, at least in some cases, droplets formed a raft before entering the circulation zone.

3.5. Thermal stresses in polycrystals

Signs of the spontaneous relief of internal stress were frequently seen when there were more than two basal flats on a particle. Cracks and even slip were visible, the deformation sometimes resulting in the partial detachment of a polycrystalline cap (Fig. 4c and l). We believe this to be an effect of thermal expansion anisotropy [26–28]. (An example in a Cd particle is seen in Fig. 5b of [1].) The only signs of distortion in bicrystals was a pinching effect along the grain boundary where this ran closest to the two flats (Fig. 4b). Although this might be an effect of solidification, the displacement is in the direction of maximum shear stress, which suggests plastic deformation. This incidentally provides further evidence that rafts occur at random on the surface.

The slip systems are not readily recognizable on the smooth, multi-dished spheres, which usually lack the orientated growth features of the monocrystals. If identification were possible an attempt might be made to calculate the cooling range from the deformation geometry and so to obtain an estimate of the solidification temperature of the droplet.

Acknowledgements

We are grateful to the S.R.C. for support for this research and to Pye Unicam (Cambridge) Ltd for access to a PSEM 500 Microscope (Figs. 3e, 4f and 4l).

References

1. E. R. BUCKLE and K. C. POINTON, *J. Mater. Sci.* **10** (1975) 365.
2. *Idem*, *Faraday Symp. Chem. Soc.* 7 (1973) 78.
3. H. JONES, *Rep. Progr. Phys.* **36** (1973) 1425.
4. E. R. BUCKLE and C. N. HOOKER, *Trans. Faraday Soc.* **58** (1962) 1939.
5. E. R. BUCKLE and K. C. POINTON, *Faraday Disc. Chem. Soc.* **61** (1976) in press.
6. P. G. PARTRIDGE, *Met. Rev.* **118** (1967) 169.
7. P. H. TILL and J. TURKEVICH, U.S.A.E.C. Rept. NYO-3435, (1956) January 15.
8. K. KIMOTO, Y. KAMIYA, N. NONOYAMA and R. UYEDA, *Jap. J. Appl. Phys.* **2** (1963) 702.
9. L. S. PALATNIK, G. V. FEDOROV and P. N. BOGATOV, *Sov. Phys.-Solid State* **8** (1966) 27.
10. K. HOMMA, *Ind. Health* 4 (1966) 129.
11. K. KIMOTO and I. NISHIDA, *Jap. J. Appl. Phys.* **6** (1967) 1047.
12. D. D. MCBRIDE and P. M. SHERMAN, *AIAA J.* **10** (1972) 1058.
13. E. O. HOGG and B. G. SILBERNAGEL, *J. Appl. Phys.* **45** (1974) 593.
14. J. D. EVERSOLE and H. P. BROIDA, *ibid* **45** (1974) 596.
15. H. HEYER, F. NIETRUCH and I. N. STRANSKI, *J. Crystal Growth* **11** (1971) 283.
16. R. KAISHEV and C. NANEV, "Growth of Crystals", edited by N. N. Sheftal (Proc. Symp. Crystal Growth, Moscow, 1966) p. 19.
17. J. P. HIRTH and G. M. POUND, "Condensation and Evaporation", *Progr. Mater. Sci.* **11** (Pergamon, London, 1963) p. 111.
18. C. NANEV and D. IWANOV, *Phys. Stat. Sol.* **23** (1967) 663.
19. B. MUTAFTSCHIEV and J. ZELL, *Surface Sci.* **12** (1968) 317.
20. W. BOAS and J. K. MACKENZIE, *Progr. Metal Phys.* **2** (1950) 90.

21. E. I. SALKOVITZ, *J. Metals* **189** (1951) 64.
22. A. KELLY and G. W. GROVES, "Crystallography and Crystal Defects" (Longman, London, 1970) appendix 3.
23. R. W. MAR and A. W. SEARCY, *J. Chem. Phys.* **53** (1970) 3076.
24. E. R. BUCKLE, *Nature* **186** (1960) 875.
25. E. R. BUCKLE and C. N. HOOKER, unpublished.
26. W. BOAS and R. W. K. HONEYCOMBE, *Proc. Roy. Soc. A* **186** (1946) 57.
27. *Idem, ibid* **188** (1947) 427.
28. *Idem, J. Inst. Metals* **73** (1947) 433.

Received 26 April and accepted 21 May 1976.